Fuzzy Self-Tuning Speed Control of an Indirect Field-Oriented Control Induction Motor Drive

Mavungu Masiala, *Student Member, IEEE*, Behzad Vafakhah, *Student Member, IEEE*, John Salmon, *Member, IEEE*, and Andrew M. Knight, *Senior Member, IEEE*

***Abstract*—The field-oriented control of induction machines is widely used in high-performance applications. However, detuning caused by parameter disturbances still limits the performance of these drives. In order to accomplish variable-speed operation, conventional PID-like controllers are commonly used. These controllers provide limited good performance over a wide range of operation, even under *ideal* field-oriented conditions. An alternate approach is to use the so-called "fuzzy" controller. In this paper, a self-tuning fuzzy controller is implemented. The proposed controller has the ability to adjust its parameters online according to the error between actual machine speed and a model reference. The scheme is compared to the conventional proportional-integral control and validated by simulation and experimental tests of both control techniques.**

***Index Terms*—Field-oriented control, fuzzy logic (FL), induction machine (IM), self-tuning, variable-speed drives.**

I. Introduction

INDIRECT field-oriented control (IFOC) operation of induction machine (IM) drives has been implemented in a wide range of industrial applications. The primary advantages of this approach are the decoupling of torque and flux characteristics and easy implementation. However, the performance of an IFOC IM drive is sensitive to the variation of the rotor time constant. A deviation between the instrumented and the actual motor values is said to "detune" the drive and results in deterioration in the dynamic torque response and the overall drive performance.

As a result of the detuning effect, recent research has included a significant effort toward the development of accurate online estimation of the rotor time constant [1]. The rotor time constant T_r is defined as the ratio of rotor inductance L_r over rotor resistance R_r, as given in

$$T_r = \frac{L_r}{R_r}. \tag{1}$$

Paper IPCSD-08-009, presented at the 2007 Industry Applications Society Annual Meeting, New Orleans, LA, September 23–27, and approved for publication in the IEEE TRANSACTIONS ON INDUSTRY APPLICATIONS by the Industrial Drives Committee of the IEEE Industry Applications Society. Manuscript submitted for review September 1, 2007 and released for publication April 14, 2008. Current version published November 19, 2008. This work was supported by the Natural Sciences and Engineering Research Council of Canada.

The authors are with the Department of Electrical and Computer Engineering, University of Alberta, Edmonton, AB T6G2V4, Canada (e-mail: masiala@ece.ualberta.ca; vafakhah@ece.ualberta.ca; salmon@ece.ualberta.ca; knight@ece.ualberta.ca).

Color versions of one or more of the figures in this paper are available online at http://ieeexplore.ieee.org.

Digital Object Identifier 10.1109/TIA.2008.2006342

Unfortunately, many of the proposed approaches are restricted in the torque–speed plane [2]. In addition, the drive performance will also be affected by other perturbations, such as load torque, rotor inertia, unmodeled dynamics, etc. [3].

Variable-speed operation is usually accomplished by PID-type speed controllers. It is well known that fixed-gain controllers may be insufficient to deal with systems subjected to severe perturbations. In this case, the controller gains must be continuously tuned according to the current trend of the system. Advanced adaptive techniques have been developed to deal with this issue, but due to their complexity, only a few have been implemented in IFOC IM drives, e.g., [3]–[5].

It can be difficult to effectively deal with machine problems through strict mathematical formulations. Fuzzy logic (FL) has emerged as a complement to conventional strict methods. Design objectives that are mathematically hard to express can be incorporated into FL controller (FLC) by linguistic rules. Recent literature has paid significant attention to the potential of FLC for the speed control of ac drives [3]–[13]. Various approaches have been developed and can be divided into two groups.

The first group focuses in improving the design and performance of the standard fixed-parameter FLC [6]–[8]. A conventional FLC is comprised of a set of rules, membership functions (MFs), and scaling gains. In standard FLCs, these parameters of the controller are fixed and selected under nominal conditions. The second group of approaches combine the advantages of FL and those of conventional adaptive techniques, particularly the use of model reference adaptive systems (MRASs), to improve the performance of the drive under severe perturbations of model parameters and operating conditions.

A special design of fuzzy rule base is proposed in [6] with rather promising results. However, if subjected to severe perturbations, the control may require online tuning of its parameters. The IM magnetization and starting procedures are used in [7] to select the best scaling gains of an FLC. The selected gains are functions of stator leakage and magnetizing reactance, and rotor inertia, which make them sensitive under parameter disturbances. To minimize the real-time computational burden of an FLC, a method based on simple MFs and rules has been implemented in [8].

MRAS algorithms require less computation and represent a good compromise between performance and cost [4]. Signal adaptation approaches based on model following error-driven fuzzy adaptation mechanisms have been proposed [5], [9]. Signal adaptation techniques are known to be slower than parameter adaptation. As a result, an FL-MRAS with the potential

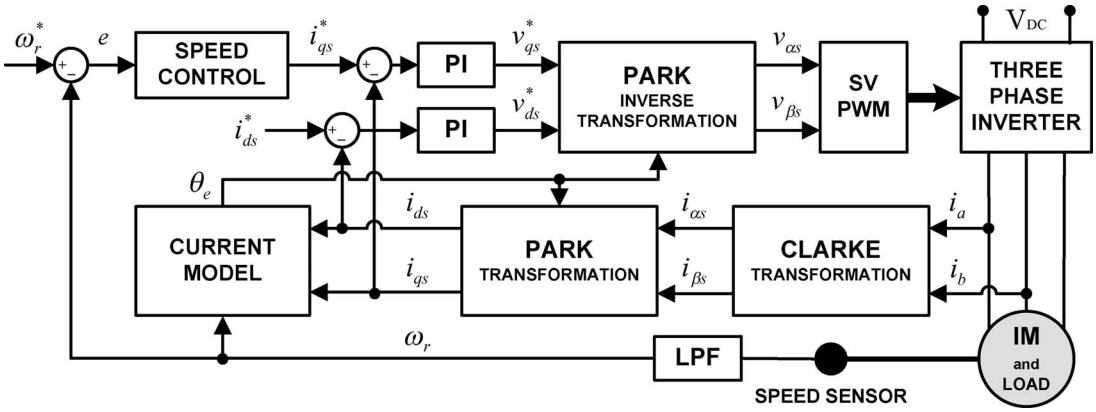

Fig. 1. Configuration of an IFOC IM drive with SVPWM.

ability to compensate for system perturbations has been successfully implemented in [9]. The structures proposed in [9] and [12] are different in their choice of adaptation targets. The adaptation target in [9] is the fuzzy rules, whereas [12] tuned the output scaling gain, providing a faster adaptive mechanism than the output signal compensation approach proposed in [5] and [9]. However, experimental tests are not provided in [12].

Several other FL-MRAS schemes have been theoretically developed [14]–[17], but few have been experimentally tested on IM drives. In many cases, the algorithms are quite complex and do not include practical constraints, such as current limits and computation burden. On the other hand, to reduce the chattering of the control effort in conventional sliding-mode control (SMC), FLC has been successfully combined with SMC and implemented in IM [3], [18], [19], [20] for position control with position encoder.

Reviewing the literature, there is relatively little experimental validation of self-tuning MRAS schemes suitable for IMs, e.g., [3]–[5], or other ac drives, e.g., [13]. Inspired by the success of the cited authors, this paper aims to improve and implement a simple but effective MRAS self-tuning FLC (STFC). Previous simulation results showed that the proposed controller is able to intelligently synthesize a single-layer FLC for the process and tune its scaling gains in real time [11]. This controller is suitable for applications, where the system must operate under uncertain conditions and when the available *a priori* information about the system is limited. Under those conditions, it is difficult to design fixed-parameter FLCs that perform sufficiently well. The control approach proposed in this paper is shown to reduce the sensitivity of the drive to motor parameter changes and load disturbances.

II. IM Drive Dynamics

The configuration of the drive investigated in this paper is shown in Fig. 1. The drive applies IFOC to a cage IM by means of a space vector pulsewidth modulation (SVPWM) current controller [21]. The simulated IM model is described in stationary reference frame and can be found in several references [2], [21].

Under ideal IFOC conditions, the rotor flux linkage is oriented along the d-axis of the motor. It follows (in the synchronously rotating reference frame) that [2]

$$\lambda_{dr} = \lambda_r^* = L_m i_{ds}^* \tag{2}$$

$$\lambda_{qr} = \frac{d\lambda_{qr}^*}{dt} = 0 \tag{3}$$

where λ_{dr} and λ_{qr} are rotor d- and q-axis flux linkages, respectively, i_{ds}^* is the stator torque component current command, and L_m is the magnetizing inductance per phase. In this case, the rotor slip speed is determined as

$$\omega_{\rm sl} = \omega_{\rm sl}^* = \frac{R_r}{L_r}\frac{i_{qs}^*}{i_{ds}^*} = \frac{1}{T_r}\frac{i_{qs}^*}{i_{ds}^*} \tag{4}$$

where $\omega_{\rm sl}$ is the rotor slip speed in electrical radians per second, i_{qs}^* is the stator flux component current command. Accordingly, the electromagnetic torque τ can be expressed as

$$\tau = \frac{3P}{2}\frac{L_m^2}{L_r} i_{ds} i_{qs} \tag{5}$$

where P is the number of pole pairs. Given the rotor flux position and two phase currents (see Fig. 1), IFOC achieves *ideal* torque and flux decoupling by means of coordinate transformations and two proportional-integral (PI) current regulators. The regulator outputs are applied to the inverse of Park transformation, the outputs of which are the stator voltages in orthogonal reference frame. The outputs of the SVPWM are the signals that drive the inverter. The current model generates the rotor flux position and is heavily dependent on T_r. The speed error is processed by the proposed STFC to generate the torque component current command i_{qs}^*.

III. Speed Controller Design

Since the proposed controller is evaluated with a conventional PI controller, the structure of the latter is briefly detailed. The proposed STFC is derived from the standard PI-type FLC (PI-FLC) and later compared with a PI controller.

A. PI Control

The PI speed controller is initially tuned by the Ziegler–Nichols method based on stability boundary [22]. It is

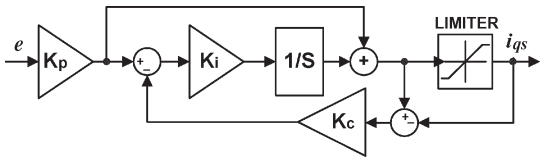

Fig. 2. PI controller with antiwindup correction term.

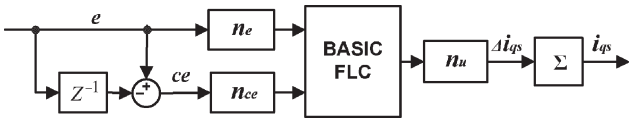

Fig. 3. PI-FLC block diagram.

subsequently tuned through simulations in order to obtain satisfactory responses. The saturation of the controller is avoided by adding a correction of the integral term (K_c) [22]. The structure of this controller is shown in Fig. 2. A similar structure is used for current regulators in Fig. 1.

B. Standard PI-FLC

Fig. 3 shows the block diagram of a standard PI-FLC, where the speed error e and its rate of change ce are the input variables; n_e, n_{ce}, and n_u are the input and output scaling gains, which will be simultaneously adjusted online to tune the proposed STFC. The basic FLC block is composed of fuzzification interface, fuzzy rules and inference mechanism, and defuzzification interface. The input/output variables used in this paper are fuzzified by five symmetrical and triangular MFs normalized in the universe of discourse between -1 and $+1$. The MFs are labeled as follows [11]: NB—negative big, NM—negative medium, ZE—zero, PM—positive medium, and PB—positive big. The MFs of adjacent fuzzy sets are complementary in the sense that the sum of membership values is one at all times. The shape of these MFs reduces the computation burden of the controller. By changing the scaling gains, the range of the input and output variables varies accordingly. The center of gravity is used to compute the output signal. The associated fuzzy rule matrices of the main PI-FLC are given in Table I. These rules were designed based on the dynamic behavior of the error signal, resulting in the symmetrical matrix. This is a general rule-based design with a 2-D phase plane. Using this method, the FLC drives the system into the so-called sliding mode [15]. In addition, this approach satisfies the three main properties of fuzzy rules: (i) completeness; (ii) consistency; and (iii) continuity. Due to its success, it has been successfully applied in many applications [2], [5], [13].

C. Proposed STFC

An STFC can be developed by applying a tuning algorithm to directly adjust the following: 1) the rules; 2) the MFs; and/or 3) the scaling gains. Techniques to tune the scaling gains in real time have received the highest priority in literature due to the influence of the gains on the performance and stability of the system [12], [23].

The real-time tuning of the scaling gains is necessary in order to maintain the desired performance of the drive. In this

TABLE I
FUZZY CONTROL RULE MATRIX

ce(k) \ e(k)	NB	NM	ZE	PM	PB
NB	NB	NB	NB	NM	ZE
NM	NB	NB	NM	ZE	PM
ZE	NB	NM	ZE	PM	PB
PM	NM	ZE	PM	PB	PB
PB	ZE	PM	PB	PB	PB

perspective, a supervised MRAS-based STFC is implemented in this paper. The desired control objective is provided at each time step. The structure of this controller is shown in Fig. 4. It consists of an IFOC with a standard PI-FLC described in Fig. 3, a model reference, and a self-tuning mechanism. The self-tuning mechanism consists of the evaluation block and the Takagi–Sugeno-type FLC (TS-FLC).

The reference model defines the desired dynamic response of the system. It is selected based on the idea of the performance achievable by the drive and to prevent excessive control action. For the IFOC of IM, a reference model can be approximated by a second order system (6), where the delay between the command and the actual currents is neglected [2], [9]. The second order reference model used in this paper is designed, following the procedure proposed in [9], and adjusted to meet the specified requirements of the investigated IM drive

$$H_m(s) = \frac{a}{s^2 + bs + a} \tag{6}$$

where s is the Laplace operator; $a = 48\,000$, and $b = 190$.

The rotor speed ω_r is compared with the reference model output ω_r' to generate the speed tracking error e_ω'. This error is first evaluated in the evaluation block. If e_ω' is within plus or minus 2 r/min, the self-tuning mechanism is not operational. If the magnitude of e_ω' exceeds the predefined range, the evaluation bloc generates the tuning error e_ω to be injected into the TS-FLC bloc. This bloc generates online weighting factors w_e, w_{ce}, and w_u that adjust the gains n_e, n_{ce}, and n_u, respectively. The tuning is performed such that the closed-loop system behaves like the reference model $H_m(s)$. The TS inference (with singleton output MFs) is selected in order to reduce the computational burden of the controller.

The effective scaling gains of the PI-FLC are derived at each step as functions of the updating factors (signals) as

$$n_e(k) = n_e(k-1)\left[\alpha \cdot w_e(k)\right] \tag{7}$$

$$n_{ce}(k) = n_{ce}(k-1)\left[\beta \cdot w_{ce}(k)\right] \tag{8}$$

$$n_u(k) = n_u(k-1)\left[\gamma \cdot w_u(k)\right]. \tag{9}$$

In (7)–(9), w_e, w_{ce}, and w_u are nonlinear fuzzy functions of tuning error, and α, β, and γ are the weight factors (constants). The fuzzy functions are limited such that the fuzzy gains remain within 1.0 per unit of the values required to maintain safe drive operation (currents are still allowed to exceed 1.0 pu for short transients).

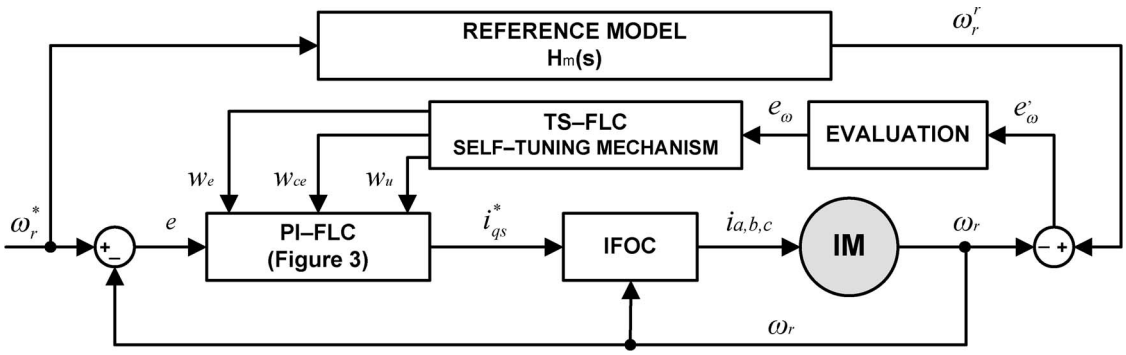

Fig. 4. Structure of the proposed STFC.

For simplicity, all the updating factors are generated using the same fuzzy lookup table. To do so, the tuning error and its rate of change are fuzzified by five symmetrical MFs, i.e., each updating gain is derived from a 5×5 TS-FLC lookup table with 25 fuzzy rules. The lookup table is constructed offline during simulations, using the load torque disturbances and sudden changes in speed reference. Moreover, the tuning is performed according to a simple predefined performance indicator. The integral of the time multiplied by the absolute value of the error (ITAE) criterion is used in (10) to "locally" optimize the controller and evaluate the degree in which the current set parameters satisfy the formulated objective. Other performance indicators can be selected as well

$$(S)_{\text{ITAE}} = \int_0^{t_{\text{stop}}} t \cdot |e_\omega(t)| \cdot dt. \tag{10}$$

If the speed error e'_ω is not within the specified allowable range, the TS-FLC operates the following type of rule:

$$\begin{aligned} &\text{IF } \{e_\omega \text{ is ZE and } ce_\omega \text{ is ZE}\}, \\ &\qquad \text{THEN } \{w_e \text{ is ZE, } w_{ce} \text{ is ZE, and } w_u \text{ is ZE}\}. \end{aligned} \tag{11}$$

In (11), the term "ZE" corresponds to the rated value. As a result, the proposed STFC does not need to know the initial scaling gains of the PI-FLC at start-up. If desired, the nominal gains can be used to reduce the starting transient. These gains can be set according to existing methods [6], [7].

It was shown in [25] and [26] that the stability of FLC closed-loop systems can be analyzed by the passivity approach, using only some general characteristics of the input–output dynamics of the systems and the input–output mapping of the controller. This approach is an extension of the classical *hyperstability* method [25]. The input–output mapping of the proposed controller can be described by the fuzzy function in the following:

$$\begin{aligned} u_1 &= \frac{\sum_{i,j} \left\lfloor \left(\mu_{E_i}(n_e \cdot e_1) \cap \mu_{E_j}(n_e \cdot e_2)\right) \cdot U_{n(i,j)}(n_u \cdot u) \right\rfloor}{\sum_{i,j} \left(\mu_{E_i}(n_e \cdot e_1) \cap \mu_{E_j}(n_e \cdot e_2)\right)} \\ &= \Phi(e_1, e_2) \end{aligned} \tag{12}$$

where e_1 is the error $e(k)$ at time instant k; e_2 is the change of error $ce(k)$; u_1 is the change of control signal $\Delta u(k) = \Delta I_{qs}(k)$; E_i, E_j, and $U_{n(i,j)}$ are the linguistic variables of e_1, e_2, and u_1, respectively; and $\cap$ is the fuzzy AND operator.

TABLE II
MOTOR NOMINAL PARAMETERS

Rated voltage (line-line) [V]	230
Rated output power [W]	2.0
Rated frequency [Hz]	60
Rated speed [rpm]	1750
Number of pole pairs	2
Stator resistance [Ω]	3.35
Rotor resistance [Ω]	3.06
Stator Leakage Inductance [mH]	21.6
Rotor Leakage Reactance [mH]	21.6
Magnetizing reactance [mH]	291

Many FLCs considered in literature (e.g., [2], [6], [10], [11], [13], [15], and [25]–[27]), including the PI-FLC described in Fig. 3, share the same distinguished input–output characteristics. These characteristics are described in [26]. This general class of FLCs has been established as sectorial fuzzy controller (SFC) [25], [27]. It is obvious that, if the PI-FLC described in Fig. 3 is SFC, then the proposed STFC will also be an SFC at all times. Using the passivity approach, the stability of SFC has been demonstrated in [26] for a single level FLC and in [27] for a multilevel FLC (self-organizing). In similar, the proposed STFC, which is an SFC, can be proven stable at all times.

IV. SIMULATION RESULTS

The effectiveness of the proposed scheme is validated by several simulations under various operating conditions and parameter disturbances. Simulations and experimental tests are performed on a 2-hp inverter-duty induction motor, with parameters summarized in Table II.

Prior to testing the control approach, the reference model performance is confirmed by considering the response of the model to a step change in reference speed, shown in Fig. 5. It can be seen that the performance of the second order model is satisfactory—faster response may result in an unachievable control objective.

The ability of the STFC to reject load disturbances was simulated at various reference speeds. The effect of applying a step increase in load (from 10% rated load to 85% rated torque) at 1.4 s and then removing the load at 2.2 s was

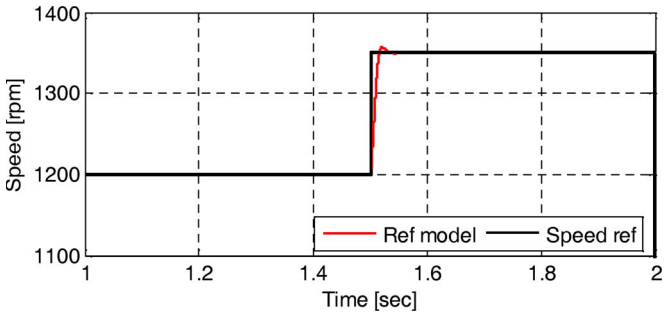

Fig. 5. Response of the second-order reference model output.

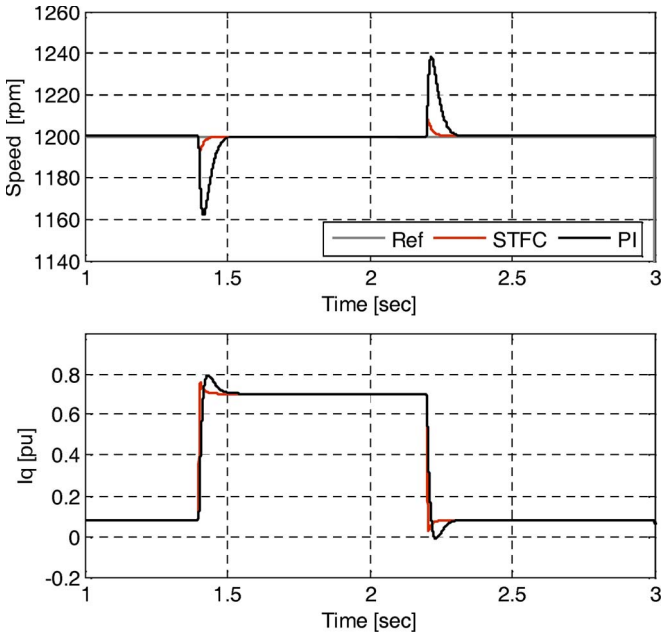

Fig. 6. Simulated response to sudden application and removal of 65% of the rated load at 1200 r/min.

investigated. The simulated responses (rotor speed and torque current component) of the STFC and PI-controlled drives are shown in Fig. 6.

Comparing the performances of the STFC and PI controller, it can be seen that the STFC offers significant improvements when compared to the fixed-parameter PI system. The STFC offers a faster response with smaller overshoot/undershoot. The STFC over/undershoot is limited to ± 7 r/min and the PI response to ± 38 r/min. The predicted q-axis currents for both systems show an acceptable overshoot, with shorter transient for the STFC.

The response of the system to a step change in command speed (at 50% initial rated load torque) is investigated next. Fig. 7 shows the results of a step change from 1200 to 1300 r/min at 2.1 s. A relatively small difference in speeds was chosen in order to minimize the effect of the current limits on the motor and drive. Analyzing the response of the systems, both systems exhibit equal settling times, but the STFC does not overshoot the command speed.

The final simulation result concerns the case of a sudden change in rotor time constant, simulated by a 50% change in rotor resistance. This is not a practical occurrence but is included to allow comparison with the results published by other

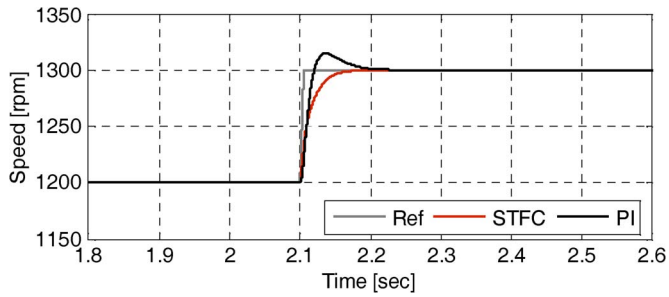

Fig. 7. Simulated response to a step change in speed at 50% of the rated load.

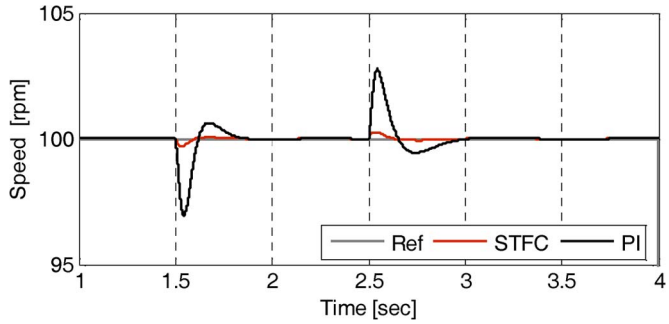

Fig. 8. Simulated response to a sudden 50% change in rotor resistance.

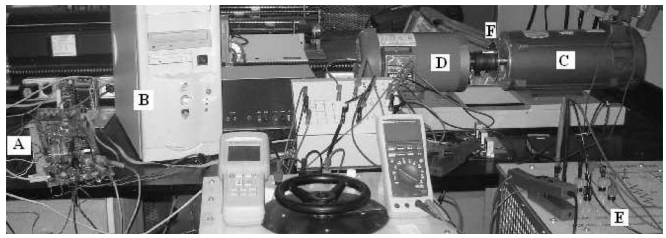

Fig. 9. Experimental test facility.

authors. The simulation assumes that the rotor time constant estimation is inaccurate at low speeds and/or low torques, where the majority of online T_r estimation methods fail to operate adequately [2]. It is important to note that the best performance of the IFOC is achieved under ideal torque and flux decoupling. The response of the system to a step increase of R_r at 100 r/min with 30% rated load torque is investigated in Fig. 8. The simulation shows that the STFC transient is significantly smaller than the PI response.

V. Experimental Results

The laboratory prototype used to verify the behavior of the STFC is shown in Fig. 9. It consists of (A) a DSP driving board, (B) control PC, and (C) a dc machine mechanically coupled to (D) an IM. The (E) switched load resistor box is used to change the loading of the IM. A 600-V/20-A 3-phase IGBT inverter is used as power stage with 330 V_{DC} rectifier output. The control board includes Analog Devices with 16-b EZ-KIT fixed-point DSP. The IM currents are measured by LEM sensors and processed by 12-b A/D converter. The speed is sensed by a 60-b/revolution sensor. It is well known that the use of speed sensors in place of position encoders may result in extra offsets, which contribute to nonideal IFOC [24].

TABLE III
CONTROL COMPUTATION TIME

	Maximum Control Time	Total Time
PI Controller	0.5 μsec	21 μsec
STFC	0.7 μsec	28 μsec

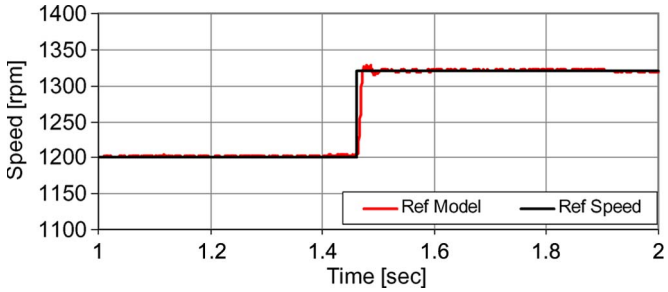

Fig. 10. DSP response of the second-order reference model.

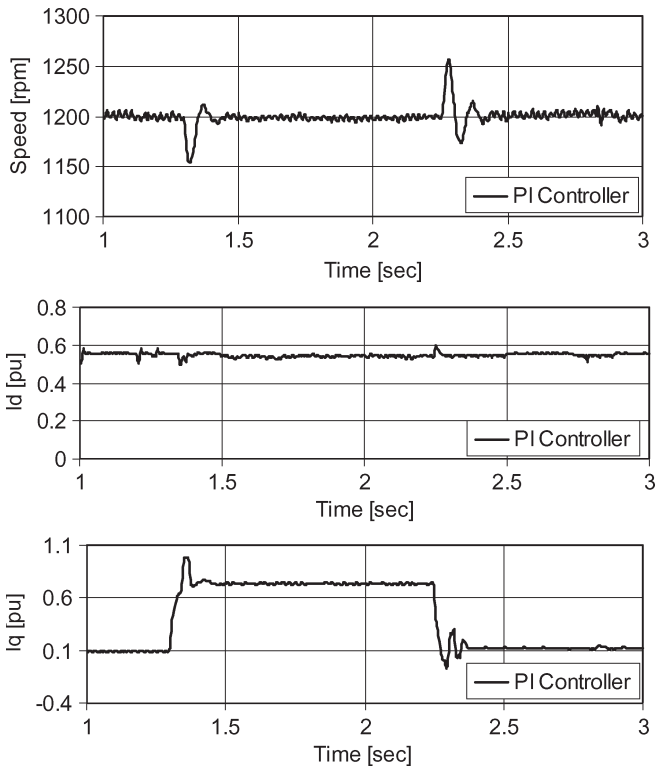

Fig. 11. Experimental response of the PI controller to a step increase of 65% rated load torque with reference speed 1200 r/min.

The control algorithms are implemented with an ADMC21992 160-MHz DSP, using assembly code. The PWM switching pattern is generated with a 10-kHz switching frequency using space vector modulation. The internal data of the DSP are displayed through an eight-channel 12-b D/A converter. The computation requirements of the control approaches are given in Table III.

As with the simulations, the implementation of the second order reference model under step change in speed references was first investigated prior to testing the rest of the control algorithm. The response is shown in Fig. 10. It can be seen that the output response of the reference model is identical to the simulated performance in Fig. 5.

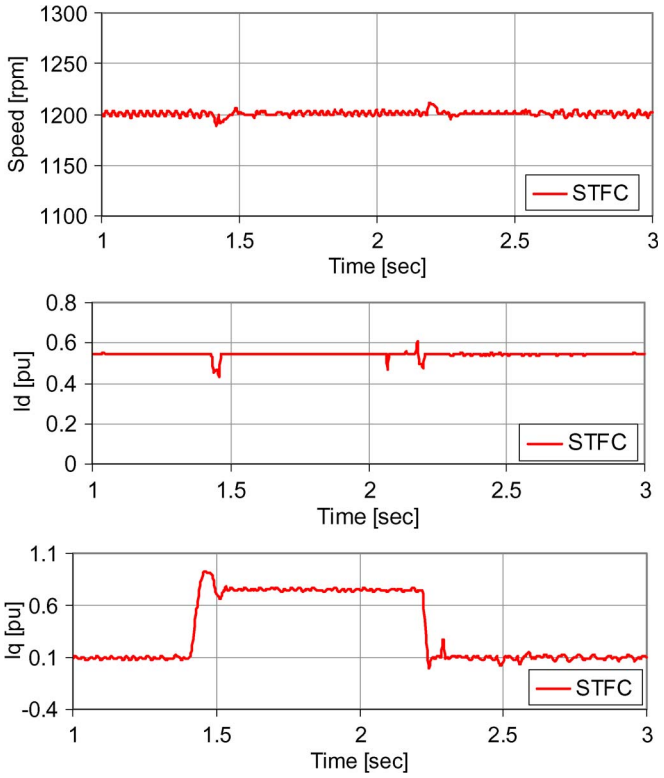

Fig. 12. Experimental response of the proposed controller (STFC) to a step increase of 65% rated load torque with a reference speed of 1200 r/min.

Investigating the ability of the drive to reject load disturbances, the drive was initially operated at 1200 r/min with 10% rated torque. A sudden step increase of 65% rated load torque (i.e., a total of 75% rated load torque) is applied at 1.3 s and 1.4 s for the PI and STFC, respectively, and then removed at 2.25 s and 2.2 s, respectively. The responses of the PI and STFC controlled drives are shown in Figs. 11 and 12, respectively.

The STFC exhibits very small undershoot and overshoot (approximately 8 r/min) than the PI (50 r/min). The responses of the actual torque component of currents show that the STFC is faster than the PI within current limits. The actual flux component currents of both controllers regained their reference values after the loading and unloading of the motor. Note that, during implementation, the loading of the motor was accomplished through the dc generator using the load box switches (see Fig. 9). Consequently, the simulated loading behaviors of the drive are slightly different than the implemented ones.

The speed tracking capabilities of the PI and STFC are investigated in Figs. 13 and 14, respectively. As the machine is initially operating in steady state at 1200 r/min with 50% rated load torque, a sudden change in reference speed, to 1300 r/min, is applied at 2.1 s. The results show that the STFC exhibits no overshoot with a fast response and confirm the simulation results shown in Fig. 7. The actual flux component currents of both controllers are able to settle down in shortly small undershoots. The actual torque component current response of the STFC is faster than that of the PI and has no undershoot.

The speed tracking capability and the load disturbance ability of the STFC are also investigated at low speed operation. The motor is initially operating at 100 r/min with 30% rated load

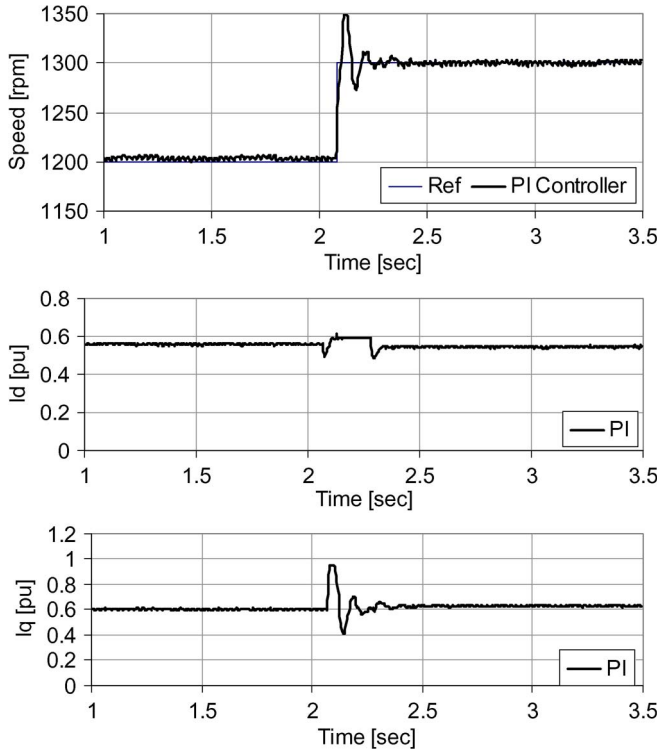

Fig. 13. Experimental response of the PI controller to a step change in speed from 1200 to 1300 r/min.

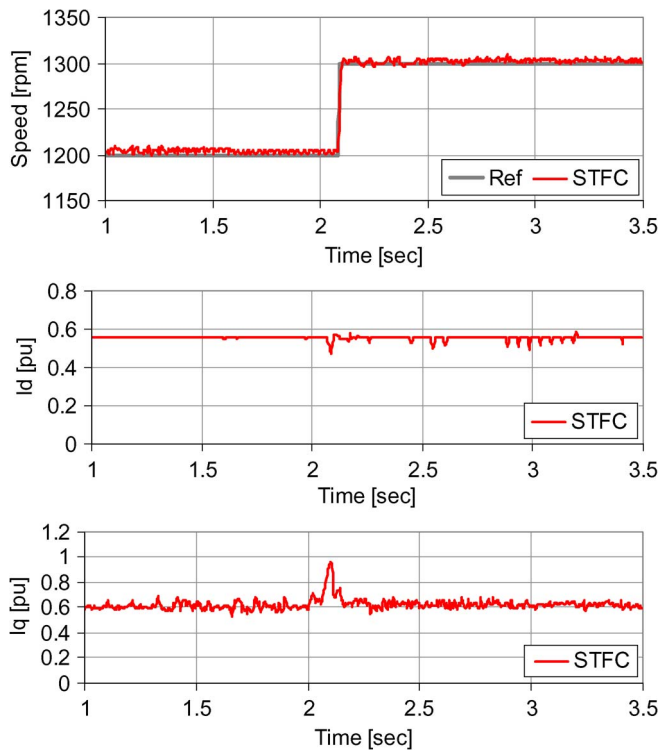

Fig. 14. Experimental response of the proposed controller (STFC) to step change in speed from 1200 to 1300 r/min.

torque. A step change in reference speed to 300 r/min is applied at 2.9 s, with a step back down to 100 r/min applied at 3.75 s. Results are shown in Fig. 15. It can be seen that the proposed controller has excellent low speed tracking performance. The

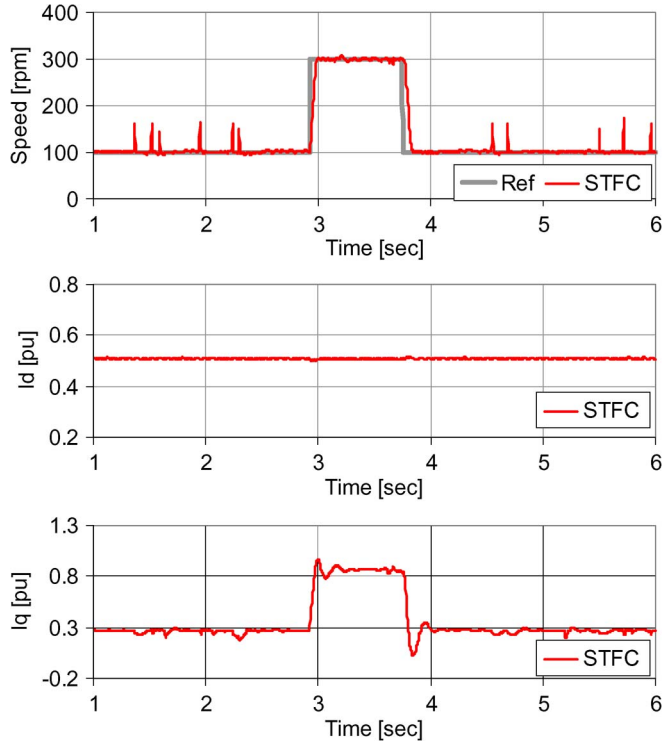

Fig. 15. Experimental response of the proposed controller (STFC) to a step change in speed from 100 to 300 r/min.

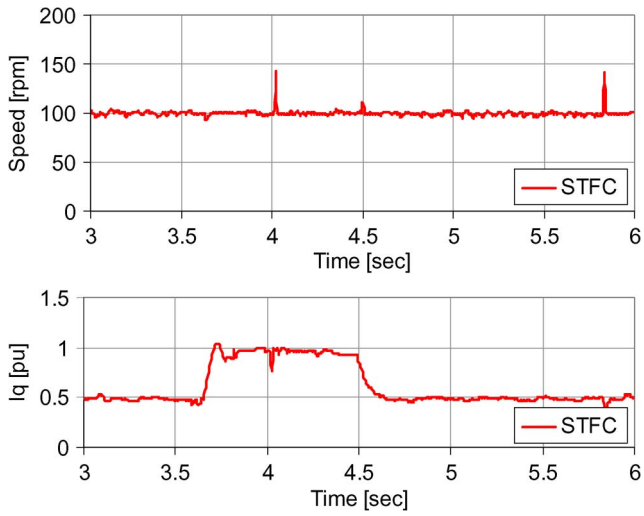

Fig. 16. Experimental response of the proposed controller (STFC) to a sudden increase and decrease of rotor resistance.

noise in the response is due to the experimental configuration: The speed sensor has a resolution of 60 b/revolution and is attached to the load dc machine. The backlash in the coupling and the slow updating of the speed signal (relative to the control loop) introduce noise and noise sensitivity. These effects are reduced at higher speeds and loads. It is possible to reduce noise with a low-pass filter on the speed signal but at the expense of transient response. Therefore, at low speed operations, a compromise between noise and transient response was required.

The final experimental results concern the case of sudden change in rotor resistance to verify the simulation result obtained in Fig. 8. As the motor is operating at 100 r/min with

30% rated load torque, the value of the rotor resistance R_r is suddenly doubled in the current model block (in Fig. 1) at 3.6 s and returned to its nominal value (reported in Table II) at 4.55 s.

Fig. 16 shows the responses of STFC speed and torque component current. It can be seen that the speed response is stable and fast, as expected from Fig. 8. This test indicates that the proposed scheme has the ability to compensate for motor parameter disturbances. However, it can also be seen that the torque current command approaches 1.0 pu even through the load is only 30% of rated. As one would expect, one could not expect to maintain stability under all conditions in the case of such a severe error. However, it is clear that the proposed approach has an excellent disturbance rejection capability.

VI. Conclusion

This paper has described the design, simulation, and test of a simple but effective STFC for the speed control of IFOC of the induction motor drives. Through a series of simulations and experimental tests, the speed tracking and disturbance rejection capabilities of the controller were verified.

Keeping in mind the requirement to minimize cost for industrial uses, the compromise between performance and computation burden is considered. This is a topic of ongoing research. Possible improvements to the approach in this paper will include methods with smaller numbers of MFs.

A key feature of the proposed scheme is the fact that the knowledge of the motor parameters is not strictly required at startup (although, in order to reduce the transient response, the rated motor parameters can be used to set the initial gains of the controller). The ability of the system to indirectly respond to parameter and load changes, without the need for computationally expensive parameter estimation, makes the approach attractive for a wide range of drive applications.

Implementing both the proposed controller and a traditional fixed-parameter PI controller, the proposed approach is shown to offer a number of performance advantages over PI controller. These advantages include smaller overshoot and faster response, even though the sampling time for current and speed control inputs is on the order of magnitude longer than for the PI system.

References

[1] H. A. Toliyat, E. Levi, and M. Raina, "A review of RFO induction motor parameter estimation techniques," *IEEE Trans. Energy Convers.*, vol. 18, no. 2, pp. 271–283, Jun. 2003.

[2] B. K. Bose, *Modern Power Electronics and AC Drives*. Upper Saddle River, NJ: Prentice-Hall, 2002.

[3] R.-J. Wai and K.-H. Su, "Adaptive enhanced fuzzy sliding-mode control for electrical servo drives," *IEEE Trans. Ind. Electron.*, vol. 53, no. 2, pp. 569–580, Apr. 2006.

[4] E. Cerruto, A. Consoli, A. Raciti, and A. Testa, "Fuzzy adaptive vector control of induction motor drives," *IEEE Trans. Power Electron.*, vol. 12, no. 6, pp. 1028–1040, Nov. 1997.

[5] K. H. Chao and C. M. Liaw, "Fuzzy robust speed controller for detuned field-oriented induction motor drive," *Proc. Inst. Electr. Eng.—Electr. Power Appl.*, vol. 147, no. 1, pp. 27–36, Jan. 2000.

[6] B. Heber, L. Xu, and Y. Tang, "Fuzzy logic enhanced speed control of an indirect field-oriented induction machine drive," *IEEE Trans. Power Electron.*, vol. 12, no. 5, pp. 772–778, Sep. 1997.

[7] F. Cupertino, A. Lattanzi, and S. Salvatoire, "A new fuzzy logic-based controller design method for DC and AC impressed-voltage drives," *IEEE Trans. Power Electron.*, vol. 15, no. 6, pp. 974–982, Nov. 2000.

[8] M. N. Uddin, T. S. Radwan, and A. Rahman, "Performances of fuzzy-logic-based indirect vector control for induction motor drive," *IEEE Trans. Ind. Appl.*, vol. 38, no. 5, pp. 1219–1225, Sep./Oct. 2002.

[9] C. M. Liaw and F. J. Lin, "Position control with fuzzy adaptation for induction servomotor drive," *Proc. Inst. Electr. Eng.—Electr. Power Appl.*, vol. 142, no. 6, pp. 397–404, Nov. 1995.

[10] L. Zhen and L. Xu, "Fuzzy learning enhanced speed control of an indirect field-oriented induction machine drive," *IEEE Trans. Control Syst. Technol.*, vol. 8, no. 2, pp. 270–278, Mar. 2000.

[11] M. Masiala and A. Knight, "Self-tuning speed controller of indirect field-oriented induction machine drives," in *Proc. XVII Int. Conf. Elect. Mach.*, Chania, Greece, Sep. 2–5, 2006, pp. 563–568.

[12] A. El Dessouky and M. Tarbouchi, "Fuzzy model reference self-tuning controller," in *Proc. 7th Int. Workshop Advanced Motion Control*, Jul. 3–5, 2002, pp. 153–158.

[13] M. Cheng, Q. Sun, and E. Zhou, "New self-tuning fuzzy PI control of a novel doubly salient permanent-magnet motor drive," *IEEE Trans. Ind. Electron.*, vol. 53, no. 3, pp. 814–821, Jun. 2006.

[14] R. K. Mudi and N. R. Pal, "A robust self-tuning scheme for PI- and PD-type fuzzy controllers," *IEEE Trans. Fuzzy Syst.*, vol. 7, no. 1, pp. 2–16, Feb. 1999.

[15] Y. Miloud, A. Miloudi, M. Mostefai, and A. Draou, "Self-tuning fuzzy logic speed controller for induction motor drives," in *Proc. IEEE Int. Conf. Ind. Technol.*, Dec. 8–10, 2004, pp. 454–459.

[16] L. Mokrani and R. Abdessemed, "A fuzzy self-tuning PI controller for speed control of induction motor drive," in *Proc. IEEE Conf. Control Appl.*, Jun. 2003, vol. 2, pp. 785–790.

[17] J. Sun, P. Su, Y. Li, and L. Li, "Application of self-adjusting fuzzy controller in a vector-controlled induction motor drive," in *Proc. 3rd IEEE Int. Conf. Power Electron. Motion Control*, Aug. 15–18, 2000, vol. 3, pp. 1197–1201.

[18] R.-J. Wai, C.-M. Kin, and C.-F. Hsu, "Hybrid control for induction servomotor drive," *Proc. Inst. Electr. Eng.—Control Theory Appl.*, vol. 149, no. 6, pp. 555–562, Nov. 2002.

[19] R.-J. Wai, C.-M. Lin, and C.-F. Hsu, "Adaptive fuzzy sliding-mode control for electrical servo drive," *Fuzzy Sets Syst.*, vol. 143, no. 2, pp. 295–310, Apr. 2004.

[20] R. J. Wai, "Fuzzy sliding-mode control using adaptive tuning technique," *IEEE Trans. Ind. Electron.*, vol. 54, no. 1, pp. 586–594, Feb. 2007.

[21] H. A. Toliyat and S. Campbell, *DSP-Based Electromechanical Motion Control*. Boca Raton, FL: CRC Press, 2004.

[22] G. F. Franklin, J. D. Powell, and A. Emami-Naeini, *Feedback Control of Dynamic Systems*. Reading, MA: Addison-Wesley, 1994.

[23] M. Braae and D. A. Rutherford, "Selection of parameters for a fuzzy logic controller," *Fuzzy Sets Syst.*, vol. 2, no. 3, pp. 185–199, Jul. 1979.

[24] D. W. Novotny and T. A. Lipo, *Vector Control and Dynamics of AC Drives*. Oxford, U.K.: Oxford Univ. Press, 1996.

[25] G. Calcev, R. Gorez, and M. De Neyer, "Passivity approach to fuzzy control systems," *Automatica*, vol. 34, no. 3, pp. 339–344, Mar. 1998.

[26] G. Calcev, "Some remarks on the stability of Mamdani fuzzy control systems," *IEEE Trans. Fuzzy Syst.*, vol. 6, no. 3, pp. 436–442, Aug. 1998.

[27] C. Xu and Y. C. Shin, "Design of a multilevel fuzzy controller for nonlinear systems and stability analysis," *IEEE Trans. Fuzzy Syst.*, vol. 13, no. 6, pp. 761–778, Dec. 2005.

Mavungu (John) Masiala (S'06) received the B.Sc. degree in engineering and technology from the Saint-Petersburg Electrotechnical University, Saint-Petersburg, Russia, in 2001, and the M.Sc. degree in applied sciences from the Université de Moncton, Moncton, NB, Canada, in 2004. He is currently working toward the Ph.D. degree in the Department of Electrical and Computer Engineering, University of Alberta, Edmonton, AB, Canada.

His research interests include fuzzy control, ac drives, and power system automatic generation control.

Mr. Masiala is a member of the Association of Professional Engineers, Geologists, and Geophysicists of Alberta.

Behzad Vafakhah (S'07) was born in Tehran, Iran, in 1976. He received the B.Sc. degree in electrical engineering from K. N. Toosi University of Technology, Tehran, in 1998, and the M.Sc. degree in electrical engineering from Sharif University of Technology, Tehran, in 2000. He is currently working toward the Ph.D. degree in the Department of Electrical and Computer Engineering, University of Alberta, Edmonton, AB, Canada, where he joined the Power Research Group in 2005.

From 2001 to 2004, he was a Research Assistant with the Power Electronics Laboratory, University of Tehran, Tehran. At the same time, he was a Design Engineer with the Abrizan Pump Company, Iran. His current research specializes in power electronics, motor drives, energy storage systems, and digital signal Processing controls.

Mr. Vafakhah is a member of the Association of Professional Engineers, Geologists, and Geophysicists of Alberta.

John Salmon (M'87) received the B.Sc. degree in engineering from Imperial College, London, U.K., in 1982, the M.Eng. degree from McGill University, Montreal, QC, Canada, in 1984, and the Ph.D. degree from Imperial College in 1987.

He joined the Department of Electrical and Computer Engineering, University of Alberta, Edmonton, AB, Canada, as an Assistant Professor in 1987, where he has been a Professor since 1996. He has conducted industrially funded power electronics research projects covering a wide range of applications, such as electronic ballasts, utility interface of wind power generators, microturbine generators using high-speed permanent-magnet generators, and medium-voltage industrial drive systems. His current research activities include industrial drive systems and their utility interface, multipulse utility rectifiers, pulsewidth-modulation (PWM) current control techniques using analog and DSP electronics, multilevel voltage-source converters for application in variable-speed drive systems, high-speed flywheel energy storage systems applied to rapid transit systems and wind power generators, multifunctional PWM converter topologies using multifunctional PWM control techniques, and phase-locked loop control techniques.

Andrew M. Knight (S'95–A'98–M'99–SM'06) received the B.A. degree in electrical and information sciences and the Ph.D. degree in electrical power engineering from the University of Cambridge, Cambridge, U.K., in 1994 and 1998, respectively.

He joined the University of Alberta, Edmonton, AB, Canada, as an Assistant Professor in 1999, where he is currently an Associate Professor in the Department of Electrical and Computer Engineering. His research is focused on the efficient utilization of electrical energy, including energy conversion, storage, and transmission. Within this field, he has particular interest in the fields of renewable energy and electrical machines and drives. In addition to his interest in the practical analysis and design of electrical systems, he also has carried out research on modeling of nonlinear magnetic systems, including both finite-element and analytical modeling techniques.